



Published in final edited form as:

Kidney Int. 2013 November ; 84(5): 895–901. doi:10.1038/ki.2013.207.

NALP3-mediated inflammation is a principal cause of progressive renal failure in oxalate nephropathy

Felix Knauf¹, John R. Asplin⁶, Ignacio Granja⁶, Insa M. Schmidt¹, Gilbert Moeckel³, Rachel David¹, Richard A. Flavell^{4,5}, and Peter S. Aronson^{1,2}

¹Department of Internal Medicine, Yale University School of Medicine, New Haven, Connecticut 06520, USA

²Department of Cellular and Molecular Physiology, Yale University School of Medicine, New Haven, Connecticut 06520, USA

³Department of Pathology, Yale University School of Medicine, New Haven, Connecticut 06520, USA

⁴Department of Immunobiology, Yale University School of Medicine, New Haven, Connecticut 06520, USA

⁵Howard Hughes Medical Institute, Yale University School of Medicine, New Haven, Connecticut 06520, USA

⁶Litholink Corporation, Chicago, Illinois 60612, USA

Abstract

Oxalate nephropathy with renal failure is caused by multiple disorders causing hyperoxaluria due to either overproduction of oxalate (primary hyperoxaluria) or excessive absorption of dietary oxalate (enteric hyperoxaluria). To study the etiology of renal failure in crystal-induced kidney disease, we created a model of progressive oxalate nephropathy by feeding mice a diet high in soluble oxalate (high oxalate in the absence of dietary calcium). Renal histology was characterized by intratubular calcium-oxalate crystal deposition with an inflammatory response in the surrounding interstitium. Oxalate nephropathy was not found in mice fed a high oxalate diet that also contained calcium. NALP3, also known as cryopyrin, has been implicated in crystal-associated diseases such as gout and silicosis. Mice fed the diet high in soluble oxalate demonstrated increased NALP3 expression in the kidney. *Nalp3*-null mice were completely protected from the progressive renal failure and death that occurred in wild-type mice fed the diet high in soluble oxalate. NALP3-deficiency did not affect oxalate homeostasis, thereby excluding differences in intestinal oxalate handling to explain the observed phenotype. Thus, progressive renal failure in oxalate nephropathy results primarily from NALP3-mediated inflammation.

Users may view, print, copy, and download text and data-mine the content in such documents, for the purposes of academic research, subject always to the full Conditions of use:http://www.nature.com/authors/editorial_policies/license.html#terms

Address correspondence: Peter S. Aronson, M.D. Department of Internal Medicine, Yale School of Medicine, 1 Gilbert Street, TAC S-255, P.O. Box 208029, New Haven, CT 06520-8029, phone: 203-785-4902, fax: 203-785-3756, peter.aronson@yale.edu.

DISCLOSURE

None of the authors has a relationship with a company with a commercial interest in the information contained in this paper.

Keywords

Oxalate; crystal nephropathy; NALP3; inflammasome

INTRODUCTION

Primary hyperoxalurias are devastating inherited diseases characterized by systemic oxalosis associated with chronic calcium-oxalate nephropathy that eventually results in end-stage renal disease.¹ Enteric hyperoxaluria due to excessive absorption of dietary oxalate can also result in oxalate nephropathy with renal failure, and has been reported in a wide variety of disorders including chronic pancreatitis,² cystic fibrosis,³ celiac disease,⁴ Crohn's disease,^{5, 6} and ingestion of a high oxalate load.⁷ Malabsorptive bariatric surgery is an increasingly common cause of enteric hyperoxaluria, which can cause oxalate nephropathy.⁸ Acute and chronic renal failure secondary to crystal nephropathy has generally been attributed to intratubular obstruction.⁹ Consequently, therapies to prevent renal failure from oxalate nephropathy have been directed principally at lowering serum and urine oxalate, such as by use of pyridoxine in some patients with primary hyperoxaluria,¹⁰ and by use of an oxalate-reduced diet and calcium supplementation in patients with enteric hyperoxaluria.^{11, 12} No therapies are yet known that blunt the effect of calcium-oxalate crystal deposition in the kidney to cause renal failure.

The term inflammasome describes a high molecular weight complex that is localized to the cytosol of cells and is part of the innate immune system.¹³ The most thoroughly described inflammasome is the nucleotide-binding domain, leucine-rich repeat inflammasome (also known as NALP3, NLRP3 or cryopyrin). Upon activation, the NALP3 proteins oligomerize, and recruit the protease caspase-1 to form the inflammasome protein complex. Activated caspase-1 cleaves the biologically inactive precursors of IL-1 β and IL-18 to generate their mature inflammatory counterparts.¹³ Several studies on crystal-related diseases support the pivotal role of the NALP3 inflammasome in translating the recognition of crystals derived from monosodium urate, silica and asbestos into inflammation and tissue injury.^{14–16} The role of NALP3 has previously been implicated in acute and chronic kidney diseases¹⁷ including obstructive uropathy¹⁸ and ischemia/reperfusion injury.^{19, 20} Based on analogy with other forms of crystal-induced inflammation, we tested the hypothesis that NALP3 plays an important role in mediating the progressive renal failure observed in a model of oxalate nephropathy induced by feeding a diet high in soluble oxalate.

RESULTS

Mice on a diet high in soluble oxalate develop renal failure

We had previously demonstrated that intestinal oxalate absorption is non-saturable and passive across the tight junction.²¹ These findings lead to the prediction that a diet high in soluble oxalate will result in increased oxalate absorption, elevated serum and urine oxalate concentrations, calcium-oxalate crystal deposition in the kidney, and renal failure. To test this prediction, we fed mice a diet high in soluble oxalate (50 μ moles sodium oxalate added per gram of virtually calcium-free diet) for 14 days. In comparison, a second group of age-

and gender-matched wild-type mice were fed the same amount of oxalate in a calcium-containing diet (50 μ moles sodium oxalate added per gram of diet containing 150 μ moles/g calcium carbonate), since dietary calcium limits absorption of ingested oxalate by precipitating oxalate in the intestinal lumen.^{22, 23} Mice fed a diet high in soluble oxalate (absence of dietary calcium) developed severe elevation of BUN (Fig. 1a) and creatinine (Fig. 1b) consistent with renal failure. In contrast, animals on the high oxalate diet in the presence of dietary calcium had normal BUN and creatinine (Fig. 1a,b).

A diet high in soluble oxalate induces oxalate nephropathy and inflammation

To confirm the presence of oxalate nephropathy in mice ingesting a diet high in soluble oxalate for 14 days, we performed polarization microscopy of kidney sections. Shown in Fig. 2a, there was profound crystal deposition in kidneys of mice fed a high oxalate diet in the absence of calcium. Examination of renal histology with hematoxylin and eosin staining (HE) revealed dilatation of the tubules with crystalline material within tubule lumens (arrows), and infiltrates of mononuclear cells in the interstitium, suggesting intense inflammation (Fig. 2c). This is consistent with findings of other investigators who have suggested that calcium-oxalate deposition in the kidney can induce tubulointerstitial damage and inflammation.²⁴ To further define the inflammatory infiltrate, we stained for the presence of macrophages/monocytes by immunocytochemistry. Indicated in Fig. 2e, macrophages/monocytes staining was strongly positive. In contrast, mice that were fed a high oxalate diet in the presence of dietary calcium showed absence of crystals on polarization microscopy (Fig. 2b), normal renal histology (Fig. 2d), and stained negative for monocytes/macrophages (Fig 2f).

NALP3 inflammasome axis is upregulated in oxalate nephropathy

As a first step to evaluate whether the NALP3-IL-1 β axis is involved in the inflammatory response to calcium-oxalate crystal deposition, *Nalp3* and IL-1 β mRNA levels were measured in kidneys of age- and gender-matched wild-type mice maintained for 6 days on an oxalate-free diet versus the diet high in soluble oxalate. Kidneys were harvested and quantitative PCR performed. Exposure to the diet high in soluble oxalate resulted in significant upregulation of *Nalp3* and IL-1 β gene expression (Fig. 3). These findings suggest that the NALP3-IL-1 β axis was upregulated in mice with oxalate nephropathy.

***Nalp3*-null mice are protected from renal failure in oxalate nephropathy**

In a next series of experiments, we placed age- and gender-matched wild-type and *Nalp3*-null mice on an oxalate- and calcium-free diet to determine baseline BUN and creatinine. We then switched the animals to the diet high in soluble oxalate (high oxalate, no calcium). In addition, we examined the protective effect of dietary calcium (high oxalate with dietary calcium) in a separate group of wild-type mice. Progression of renal failure was measured longitudinally by measuring plasma creatinine and BUN via retroorbital blood collections. Wild-type mice placed on a diet high in soluble oxalate demonstrated progressive renal failure over the following 18-day period as indicated by rising BUN (Fig. 4a) and creatinine (Fig. 4b). In contrast, *Nalp3*-null mice demonstrated stable BUN and creatinine. Similarly, the addition of calcium to a high oxalate diet protected from oxalate nephropathy.

Nalp3-deficiency does not affect dietary oxalate homeostasis

Our observation that *Nalp3*-null mice are protected from oxalate nephropathy was observed by use of a total body knock-out.²⁵ It is possible that the protection from oxalate nephropathy in *Nalp3*-null mice may be secondary to differences in dietary oxalate absorption due to altered inflammation in the intestine. Therefore, we measured the response of urinary oxalate excretion to ingestion of a diet high in soluble oxalate in wild-type and *Nalp3*-null mice at early time points (days 1, 3 and 6). As shown in Fig. 5a, urinary oxalate levels increased about 15-fold from baseline following a switch from an oxalate-free to a high soluble oxalate diet. Urinary oxalate excretion was identical in wild-type and *Nalp3*-null mice, thus excluding differences in intestinal oxalate handling or dietary intake to explain the observed phenotype. Similarly, plasma oxalate levels increased 30-fold in wild-type and *Nalp3*-null mice following a switch to a diet high in soluble oxalate. At six days there was a trend towards higher plasma oxalate concentrations in wild-type mice, which may be the consequence of reduced oxalate clearance in the setting of progressive renal failure observed in wild-type mice (Fig. 4 a,b).

Nalp3-deficiency does not affect initial renal crystal deposition

In addition to the above studies on the kinetics of oxalate absorption, we performed polarization microscopy of kidney sections to evaluate crystal deposition at two time points after mice were switched to the diet high in soluble oxalate. In preliminary studies we observed that there was a gender difference in crystal deposition in wild-type mice, with greater deposition in male mice. To reduce this source of variability, these studies on the time course of crystal deposition were performed in age-matched male mice only. Representative sections are shown in Fig. 6 a–d, and quantification of crystal deposition is summarized in Fig. 6 e. Consistent with the observation described above that wild-type and *Nalp3*-null mice have similar levels of plasma oxalate after 3 days on the diet with high soluble oxalate, crystal deposition in the kidney at this time point was also identical in both groups of mice, as shown in Fig. 6. However, at the 6-day time point there was greatly reduced crystal deposition in the kidneys of *Nalp3*-null compared to wild-type mice. One possibility to explain these findings is that Nalp3-mediated inflammation promotes crystal deposition. However, as indicated in Figs. 4b and 5b, at six days there is significantly reduced renal function and a trend to higher plasma oxalate in wild-type mice compared to *Nalp3*-null mice. It is therefore possible that the difference in renal crystal deposition between the two groups of mice is due to the higher plasma oxalate resulting from reduced renal function in the wild-type compared to *Nalp3*-null mice.

Nalp3-deficiency reduces but does not eliminate renal inflammation

At the same 6-day time point after male mice were switched to a diet high in soluble oxalate, we stained kidney sections for the presence of macrophages/monocytes by immunocytochemistry, as illustrated in Fig. 7. Representative sections are shown in Fig. 7 a–b, and quantification of staining is summarized in Fig. 7c. We observed that whereas there was widespread positive staining for macrophage/monocytes with enhanced staining in the cortico-medullary junction in the kidneys of wild-type mice, there were limited foci of strong staining in *Nalp3*-null mice.

***Nalp3*-null mice are protected from high oxalate diet induced mortality**

In order to examine the effect of oxalate nephropathy on mortality we continued to follow the wild-type and *Nalp3*-null mice placed on the diets described above for 30 days. Animals were assessed on a daily basis and closely observed for clinical signs of severe disease. The 30-day mortality of wild-type mice placed on the diet high in soluble oxalate was 100% (Fig. 8a). Given the rising creatinine observed over time (Fig. 4 a,b), death likely occurred following progressive renal insufficiency, but the contribution of inflammation in other organ systems cannot be excluded. In contrast, *Nalp3*-null mice showed 100% survival at 30 days as they were protected from progressive renal insufficiency. Similarly, addition of dietary calcium to a high oxalate diet resulted in 100% survival at 30 days. Plasma oxalate values were compared in surviving mice at the 30-day time point. Shown in Fig. 8b, dietary calcium completely protected against hyperoxalemia in wild-type mice ingesting a high oxalate diet. In contrast, *Nalp3*-null mice had persistent extreme hyperoxalemia at the 30-day time point, yet still were completely protected against mortality induced by ingestion of the diet high in soluble oxalate. Nevertheless, while the protective effect of dietary calcium against oxalate nephropathy in wild-type mice was completely maintained for 30-days as reflected by normal BUN and creatinine values (Fig. 8c), significant elevation of creatinine was detected in *Nalp3*-null mice. Thus, *Nalp3*-deficiency greatly retards but does not completely prevent progressive oxalate nephropathy over this very prolonged time period.

DISCUSSION

The existing paradigm has been that renal failure in crystal nephropathy is largely secondary to intraluminal obstruction leading to increased tubular pressure and loss of kidney function.⁹ Our findings that *Nalp3*-deficient mice are greatly protected from the progressive renal failure and death that results from enteric hyperoxaluria suggest that the inflammasome is of major importance in the loss of kidney function that occurs in oxalate-induced kidney disease, an important example of crystal nephropathy.

While our paper was in preparation, another study of protection against oxalate-induced renal inflammation in *Nalp3*-null mice was reported.²⁶ This study used a model of acute oxalate loading by intraperitoneal injection resulting in peak renal injury at 24 hours, which resolved within 7 days even in wild-type mice. Renal injury was dependent on mononuclear cell infiltration and was partially ameliorated in mice deficient in MyD88, NLRP3, ASC, caspase-1, IL-1R, or IL-18. Our work extends these observations by use of a model of chronic enteric oxalate loading resulting in progressive renal failure and death over a 30-day period. Even with this prolonged period of oxalate loading, there was marked protection against oxalate-induced renal failure and complete protection against death in *Nalp3*-null mice.

Because intestinal oxalate absorption is passive and paracellular²¹ and because inflammatory cytokines can alter tight junction permeability,²⁷ it was important to examine whether the protection in *Nalp3*-null mice against renal failure induced by a diet high in soluble oxalate might be due to reduced oxalate absorption. Accordingly, our work included measurements of serum and urine oxalate to verify that there was no difference in the absorbed oxalate load between wild-type and *Nalp3*-null mice. Similarly, there was no

difference in the initial level of crystal deposition between wild-type and *Nalp3*-null mice. Of note, the plasma levels of oxalate resulting from oxalate loading in our study, 40–60 μM , exceed the threshold of 30 μM generally associated with systemic oxalosis,²⁸ underscoring the remarkable and prolonged protection against oxalate-induced renal failure observed in *Nalp3*-null mice.

In summary, we have developed a model of oxalate nephropathy by feeding mice a diet high in soluble oxalate with development of renal failure and death. Using this model we have demonstrated that *Nalp3*-null mice are completely protected from progressive renal impairment and mortality as compared to wild-type mice. This work emphasizes the potential value of anti-inflammatory therapies to slow the rate of progression of oxalate nephropathy in patients with inherited and acquired forms of hyperoxaluria.

MATERIALS AND METHODS

Animals and diets

All measurements were performed on 12-week old gender-matched wild-type and *Nalp3*-null mice.²⁵ The generation of mice deficient in NALP3 has been described previously.²⁵ NALP3-deficient mice were fully backcrossed to C57BL/6 background. Age- and gender-matched C57BL/6 mice from Jackson Laboratory were used as wild-type controls. Mouse synthetic diets were obtained from Harlan (Madison, WI, USA). A high oxalate diet was prepared by adding sodium-oxalate (50 $\mu\text{moles/g}$) to a virtually calcium-free diet (TD. 95027), or to a diet containing calcium added as calcium carbonate (150 $\mu\text{moles/g}$ in diet TD.97191). In some experiments, animals were fed the oxalate- and calcium-free diet alone (TD. 95027). All animal procedures were approved by the Yale University Institutional Animal Care and Use Committee (protocol #2011-07258).

Measurement of BUN, creatinine and oxalate

Mouse plasma was collected via retroorbital bleed collections. Plasma BUN was measured with the COBAS MIRA system (Roche Diagnostics, Indianapolis, IN). Plasma creatinine values were measured by the Mouse Metabolic Phenotyping Center at Yale by use of LC/MS/MS (liquid-chromatography/tandem mass spectrometry) using Hamilton PRP-X200 column interfaced to an API-3000.²⁹ Oxalate was measured by ion chromatography using a Dionex ICS 2000 system (Dionex Corporation Sunnyvale CA) equipped with an AG-22 guard column and AS-22 analytical column in series. The mobile phase was potassium tetraborate at a flow rate of 1.2 ml/minute. Ion peaks were detected using a conductivity meter with the eluent background conductivity suppressed using an anion self-regenerating suppressor (ASRS Ultra II, Dionex Corp). Plasma oxalate was measured by diluting the plasma ultrafiltrate with water and loading onto the column with a 200 μl injection loop. For urine samples, an ultrafiltrate was prepared using a 10 kD centrifugal ultrafiltration device. The samples were loaded using a 50 μl injection loop. Urine dilutions varied from 1:20 to 1:50 and plasma dilutions varied from 1:3 to 1:12, so that the peak area fell in the range of the calibration. Chromeleon Software (Version 6.5, Dionex Corp) was used to measure peak area and calculate the oxalate concentration.

Renal histology

Mouse kidneys were routinely processed for paraffin-embedding and positioned in order to obtain complete cross sections of the kidney at the level of the renal papilla. Serial sections were cut at 4 μ m and stained with hematoxylin and eosin for routine histological examination. Kidney sections were scanned using polarization microscopy with a Nikon TE2000U inverted microscope and Meta-Morph software (Scion Inc, USA). Quantification of calcium-oxalate crystal deposition was performed by scanning whole kidneys under polarized light, and setting a pixel intensity threshold that identifies crystals separate from background tissue. Total pixels above this threshold are expressed as a percentage of total tissue pixels, thereby normalizing to kidney surface area. An avidin-biotin immunoperoxidase method was used with a monoclonal antibody directed against macrophages/monocytes (F4/80; clone BM8, Abcam, # 16911). In order to quantify F4/80 staining in kidney sections, whole kidney sections were scanned, peroxidase positive areas (dark staining) were outlined by an observer blinded to the experimental conditions, and then expressed as percent of total surface area using Meta-Morph software (Scion Inc, USA).³⁰

Analysis of mRNA/Real time polymerase chain reaction (qPCR)

Kidney RNA was extracted with an RNeasy Mini kit (Qiagen) and reverse transcribed. Gene expression analysis was determined by quantitative real-time PCR using an iCycler iQ (Bio-Rad) and normalized to mouse Hprt1.³¹ The following primers were used with Cyber Green: NALP3 Fw: CCACAGTGTAACCTTGCAGAAGC Rev: GGTGTGTGAAGTTCTGGTTGG; IL-1 β Fw: TTCCTTGTGCAAGTGTCTGAAG Rev: CACTGTCAAAGGTGGCATT; HPRT Fw: CAGTAC AGCCCCAAAATGGT Rev: CAAGGGCATATCCAACAACA. Data are expressed using the comparative threshold cycle (dCt) method and mRNA ratios are given by 2^{-dCT} .

Statistical analysis

Results are given as the mean \pm S.E. for the indicated number of experiments. For analyses, we performed unpaired Student's t-tests (Prism 6.0 program, Graphpad Software) as well as ANOVA and Duncan multiple range tests using SAS 9.3 for Windows (SAS Institute Inc., Cary, NC). Survival analysis, using Kaplan-Meier curves and Mantel-Cox tests for significance, was also performed (Prism 6.0, Graphpad Software). A Type I error of 0.05 (two-tailed) was used as the level of statistical significance for all analyses.

Acknowledgments

This work was supported by NIH grant R37DK33793, the George M. O'Brien Kidney Center at Yale (P30DK079310), the Mouse Metabolic Phenotyping Center at Yale (U24DK059635), and a postdoctoral research fellowship to F.K. from the National Kidney Foundation. We thank Chengcheng Jing and Thecla Abbiati for providing and breeding *Nalp3*-null mice, and Lonnette Diggs for assistance with mouse plasma collections.

References

1. Hoppe B, Langman CB. A United States survey on diagnosis, treatment, and outcome of primary hyperoxaluria. *Pediatr Nephrol.* 2003; 18:986–991. [PubMed: 12920626]

2. Cartery C, Faguer S, Karras A, et al. Oxalate nephropathy associated with chronic pancreatitis. *Clin J Am Soc Nephrol.* 2011; 6:1895–1902. [PubMed: 21737848]
3. Lefaucheur C, Nochy D, Amrein C, et al. Renal histopathological lesions after lung transplantation in patients with cystic fibrosis. *Am J Transplantation.* 2008; 8:1901–1910.
4. Capolongo G, Abul-Ezz S, Moe OW, et al. Subclinical celiac disease and crystal-induced kidney disease following kidney transplant. *Am J Kidney Dis.* 2012; 60:662–667. [PubMed: 22739230]
5. Mandell I, Krauss E, Millan JC. Oxalate-induced acute renal failure in Crohn's disease. *Am J Med.* 1980; 69:628–632. [PubMed: 7424952]
6. Hueppelshaeuser R, von Unruh GE, Habbig S, et al. Enteric hyperoxaluria, recurrent urolithiasis, and systemic oxalosis in patients with Crohn's disease. *Pediatr Nephrol.* 2012; 27:1103–1109. [PubMed: 22366809]
7. Chen CL, Fang HC, Chou KJ, et al. Acute oxalate nephropathy after ingestion of star fruit. *Am J Kidney Dis.* 2001; 37:418–422. [PubMed: 11157385]
8. Nasr SH, D'Agati VD, Said SM, et al. Oxalate nephropathy complicating Roux-en-Y Gastric Bypass: an underrecognized cause of irreversible renal failure. *Clin J Am Soc Nephrol.* 2008; 3:1676–1683. [PubMed: 18701613]
9. Perazella MA. Crystal-induced acute renal failure. *Am J Med.* 1999; 106:459–465. [PubMed: 10225250]
10. Hoppe B. An update on primary hyperoxaluria. *Nature reviews Nephrology.* 2012; 8:467–475. [PubMed: 22688746]
11. Worcester EM. Stones from bowel disease. *Endocrinol Metab Clin North Am.* 2002; 31:979–999. [PubMed: 12474641]
12. Worcester EM, Coe FL. Clinical practice. Calcium kidney stones. *The New England Journal of Medicine.* 2010; 363:954–963. [PubMed: 20818905]
13. Gross O, Thomas CJ, Guarda G, et al. The inflammasome: an integrated view. *Immunological Reviews.* 2011; 243:136–151. [PubMed: 21884173]
14. Martinon F, Petrilli V, Mayor A, et al. Gout-associated uric acid crystals activate the NALP3 inflammasome. *Nature.* 2006; 440:237–241. [PubMed: 16407889]
15. Cassel SL, Eisenbarth SC, Iyer SS, et al. The Nalp3 inflammasome is essential for the development of silicosis. *Proc Natl Acad Sci U S A.* 2008; 105:9035–9040. [PubMed: 18577586]
16. Dostert C, Petrilli V, Van Bruggen R, et al. Innate immune activation through Nalp3 inflammasome sensing of asbestos and silica. *Science.* 2008; 320:674–677. [PubMed: 18403674]
17. Anders HJ, Muruve DA. The inflammasomes in kidney disease. *J Am Soc Nephrol.* 2011; 22:1007–1018. [PubMed: 21566058]
18. Vilaysane A, Chun J, Seamone ME, et al. The NLRP3 inflammasome promotes renal inflammation and contributes to CKD. *Journal of the American Society of Nephrology: JASN.* 2010; 21:1732–1744. [PubMed: 20688930]
19. Shigeoka AA, Mueller JL, Kambo A, et al. An inflammasome-independent role for epithelial-expressed Nlrp3 in renal ischemia-reperfusion injury. *J Immunol.* 2010; 185:6277–6285. [PubMed: 20962258]
20. Iyer SS, Pulskens WP, Sadler JJ, et al. Necrotic cells trigger a sterile inflammatory response through the Nlrp3 inflammasome. *Proc Natl Acad Sci U S A.* 2009; 106:20388–20393. [PubMed: 19918053]
21. Knauf F, Ko N, Jiang Z, et al. Net intestinal transport of oxalate reflects passive absorption and SLC26A6-mediated secretion. *J Am Soc Nephrol.* 2011; 22:2247–2255. [PubMed: 22021714]
22. Hess B, Jost C, Zipperle L, et al. High-calcium intake abolishes hyperoxaluria and reduces urinary crystallization during a 20-fold normal oxalate load in humans. *Nephrol Dial Transplant.* 1998; 13:2241–2247. [PubMed: 9761503]
23. Holmes RP, Goodman HO, Assimos DG. Contribution of dietary oxalate to urinary oxalate excretion. *Kidney Int.* 2001; 59:270–276. [PubMed: 11135080]
24. Khan SR. Crystal-induced inflammation of the kidneys: results from human studies, animal models, and tissue-culture studies. *Clin Exp Nephrol.* 2004; 8:75–88. [PubMed: 15235923]

25. Jin C, Frayssinet P, Pelker R, et al. NLRP3 inflammasome plays a critical role in the pathogenesis of hydroxyapatite-associated arthropathy. *Proc Natl Acad Sci U S A*. 2011; 108:14867–14872. [PubMed: 21856950]
26. Mulay SR, Kulkarni OP, Rupanagudi KV, et al. Calcium oxalate crystals induce renal inflammation by NLRP3-mediated IL-1beta secretion. *J Clin Invest*. 2013; 123:236–246. [PubMed: 23221343]
27. Watson CJ, Hoare CJ, Garrod DR, et al. Interferon-gamma selectively increases epithelial permeability to large molecules by activating different populations of paracellular pores. *Journal of Cell Science*. 2005; 118:5221–5230. [PubMed: 16249235]
28. Hoppe B, Kemper MJ, Hvizd MG, et al. Simultaneous determination of oxalate, citrate and sulfate in children's plasma with ion chromatography. *Kidney Int*. 1998; 53:1348–1352. [PubMed: 9573551]
29. Takahashi N, Boysen G, Li F, et al. Tandem mass spectrometry measurements of creatinine in mouse plasma and urine for determining glomerular filtration rate. *Kidney Int*. 2007; 71:266–271. [PubMed: 17149371]
30. Hopfer H, Holzer J, Hunemörder S, et al. Characterization of the renal CD4+ T-cell response in experimental autoimmune glomerulonephritis. *Kidney Int*. 2012; 82:60–71. [PubMed: 22437418]
31. Ko N, Knauf F, Jiang Z, et al. Sat1 is dispensable for active oxalate secretion in mouse duodenum. *Am J Physiol Cell Physiol*. 2012; 303:C52–57. [PubMed: 22517357]

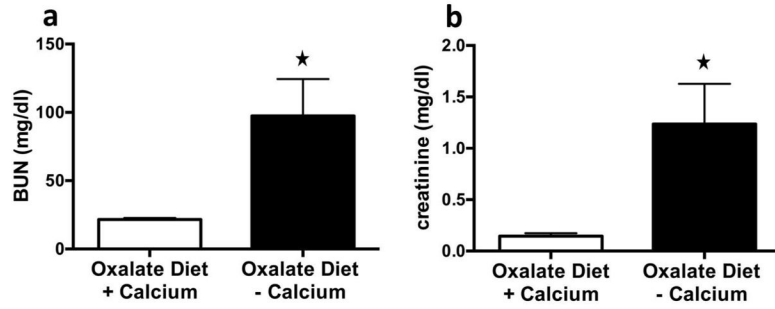


Figure 1. Wild-type mice fed a high oxalate diet in the absence of calcium develop renal failure (a) BUN and (b) creatinine were measured in wild-type mice placed for 14 days on a diet high in soluble oxalate (50 μ moles sodium oxalate added per gram of virtually calcium-free diet) or fed the same amount of oxalate in a calcium-containing diet (50 μ moles sodium oxalate added per gram of diet containing 150 μ moles/g calcium carbonate). Data expressed as the means \pm SEM; n=3 per group; p< 0.05.

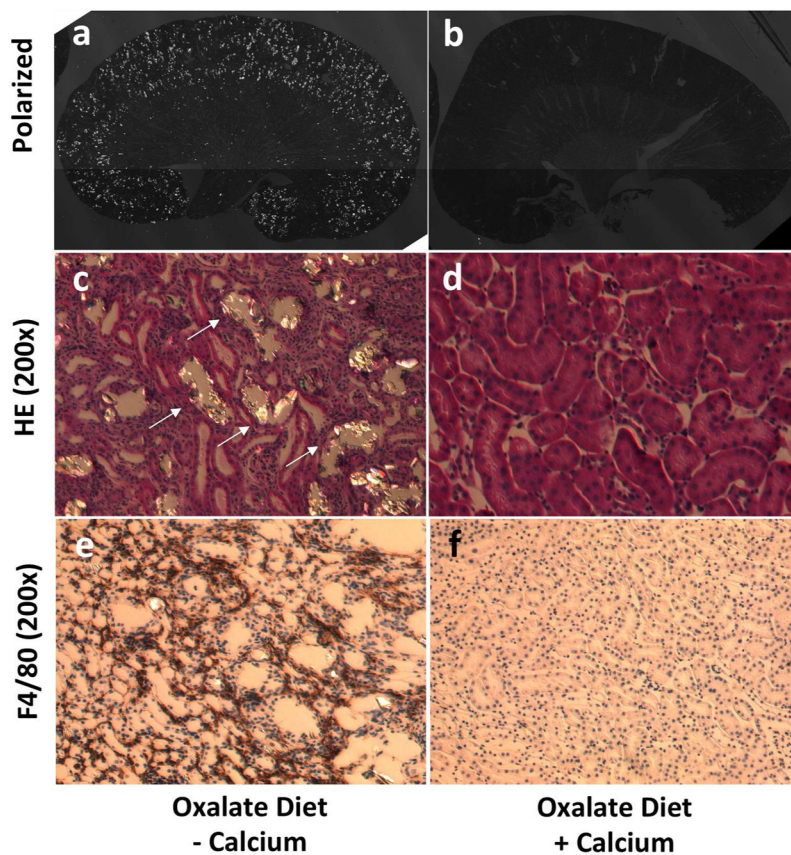


Figure 2. Wild-type mice fed a diet high in soluble oxalate develop oxalate nephropathy and inflammation

(a) Polarization microscopy of whole mouse kidneys of mice fed a high oxalate diet for 14 days in the absence of calcium demonstrates crystal deposition in the cortex and cortico-medullary junction while (b) animals placed on a high oxalate diet in the presence of calcium show no crystal deposition. (c) Hematoxylin and eosin (HE) staining reveals crystals (arrow) lining the lumen of dilated and flattened tubules with surrounding inflammation noted by the presence of mononuclear cells in mice fed an oxalate diet in the absence of dietary calcium. 200x. (d) Normal renal parenchyma in mice fed a high oxalate diet in the presence of calcium. 200x. (e) F4/80 staining for macrophages/monocytes is positive (dark color) in mice fed a high oxalate diet in the absence of calcium. 200x. (f) F4/80 staining is negative in mice fed an oxalate diet in the presence of calcium. 200x. n=3 per group, representative images are shown.

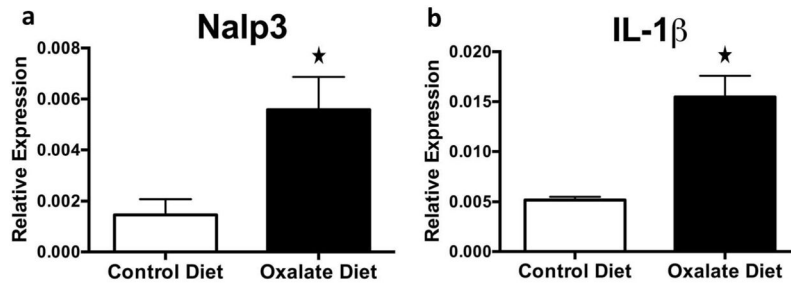


Figure 3. Nalp3 and IL-1 β mRNA levels are increased in kidneys of mice fed a high oxalate diet (a) Nalp3 and (b) IL-1 β mRNA was measured in wild-type mice maintained on a control diet (no oxalate) versus high soluble oxalate diet (50 μ moles sodium oxalate added per gram) for 6 days. Data expressed as the means \pm SEM; n=3 for control diet, n=4 for oxalate diet; p< 0.05.

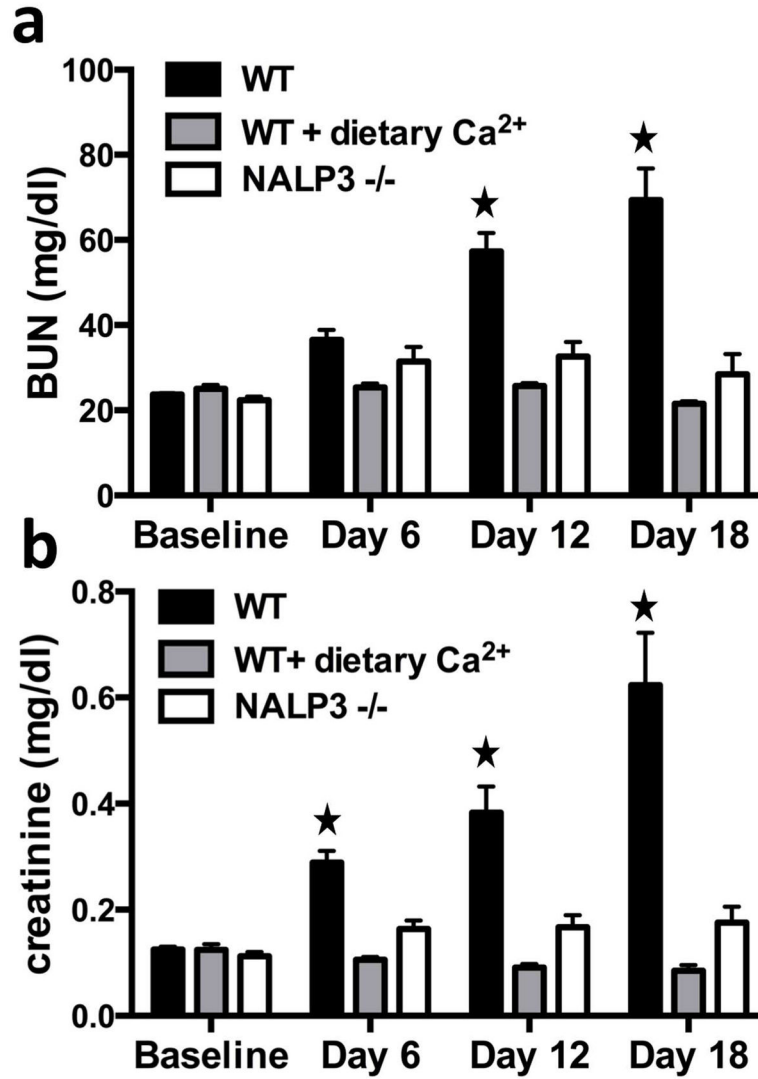


Figure 4. *Nalp3*-deficiency or dietary calcium prevents progressive oxalate nephropathy (a) BUN and (b) creatinine were measured in age- and gender-matched wild-type and *Nalp3*-null mice on an oxalate and calcium free diet to determine baseline BUN and creatinine. Animals were then switched to a diet high in soluble oxalate. In addition, a separate group of wild-type mice were fed a high oxalate diet with calcium. Data expressed as means \pm SEM; n=12 (6 male/6 female) *Nalp3*-null and wild-type mice fed the diet high in soluble oxalate; n=6 (3 male/3 female) wild-type mice fed high oxalate with calcium. There was no statistically significant difference at baseline for BUN and creatinine (p=0.70). Mean serum BUN was significantly higher in the wild-type mice fed a high oxalate diet than either other group at days 12 and 18, and for creatinine at days 6, 12 and 18 via Duncan tests (p-values <0.0001 by ANOVA).

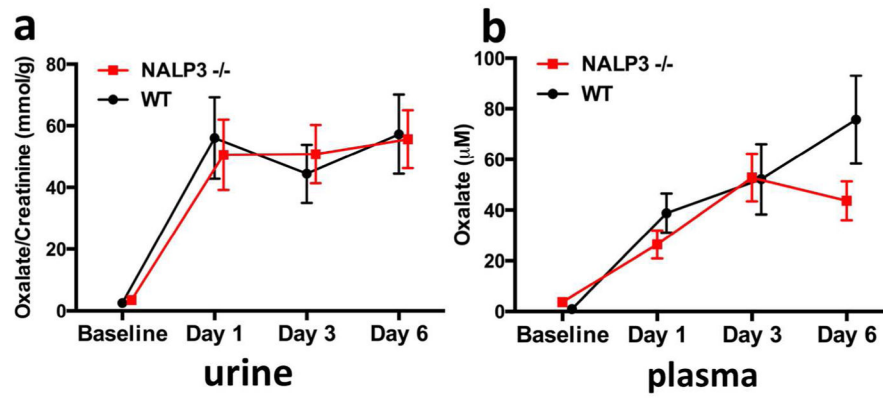


Figure 5. Nalp3-deficiency does not affect oxalate homeostasis

(a) Urinary oxalate/creatinine ratio and (b) Plasma oxalate increased about 15-fold and 30-fold respectively from baseline following a switch from an oxalate-free to a diet high in soluble oxalate. Urinary oxalate excretion was identical in age and gender-matched wild-type and *Nalp3*-null mice. Data expressed as means \pm SEM; n= 2 at baseline, n=4 at day 1, n=5 at days 3 and 6; p>0.05 each time point.

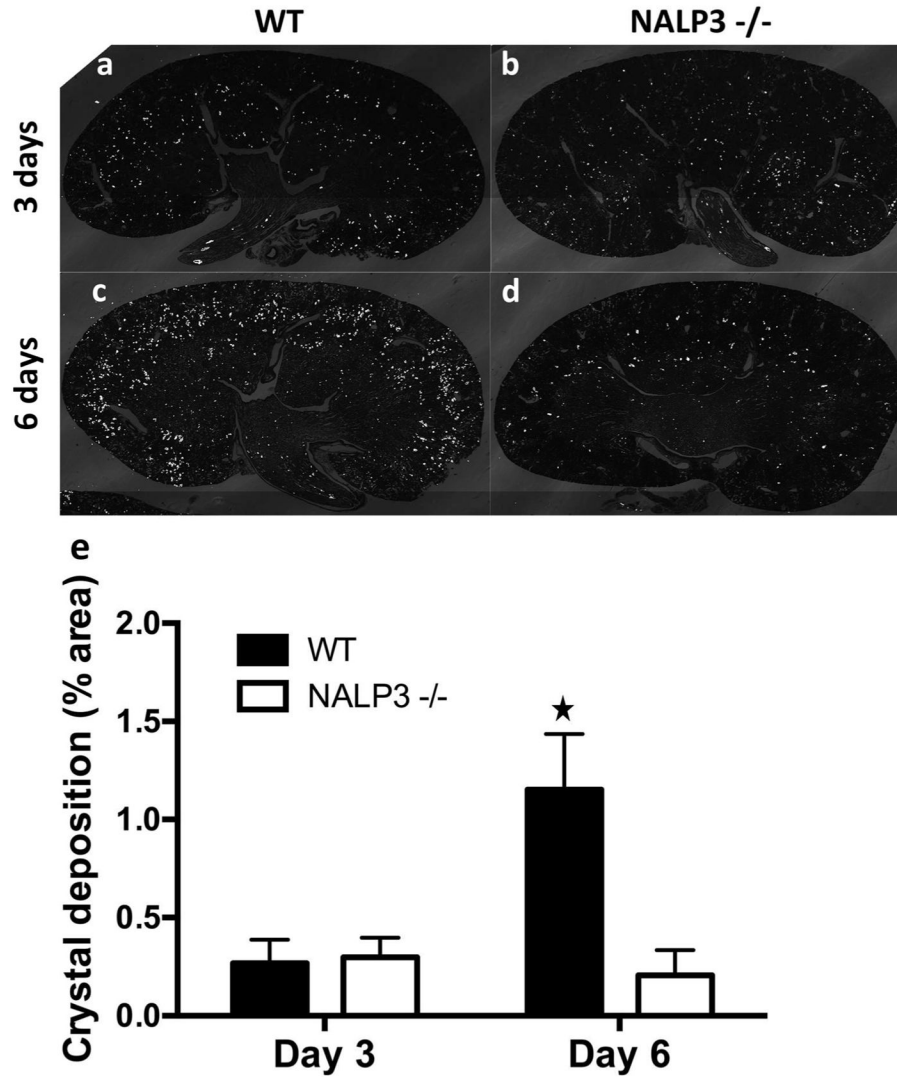


Figure 6. *Nalp3*-deficiency does not affect initial renal crystal deposition

(a) Polarization microscopy of whole mouse kidneys of wild-type mice fed a high oxalate diet in the absence of calcium demonstrated equal amounts of crystal deposition compared with (b) *Nalp3*-null mice at 3 days. (c) Crystal deposition was increased in wild-type mice compared with (d) *Nalp3*-null mice after 6 days. (e) Crystal quantification expressed per kidney surface area in wild-type and *Nalp3*-null mice. Data expressed as the means \pm SEM; n=3 male mice per group; p<0.05. Representative images are shown.

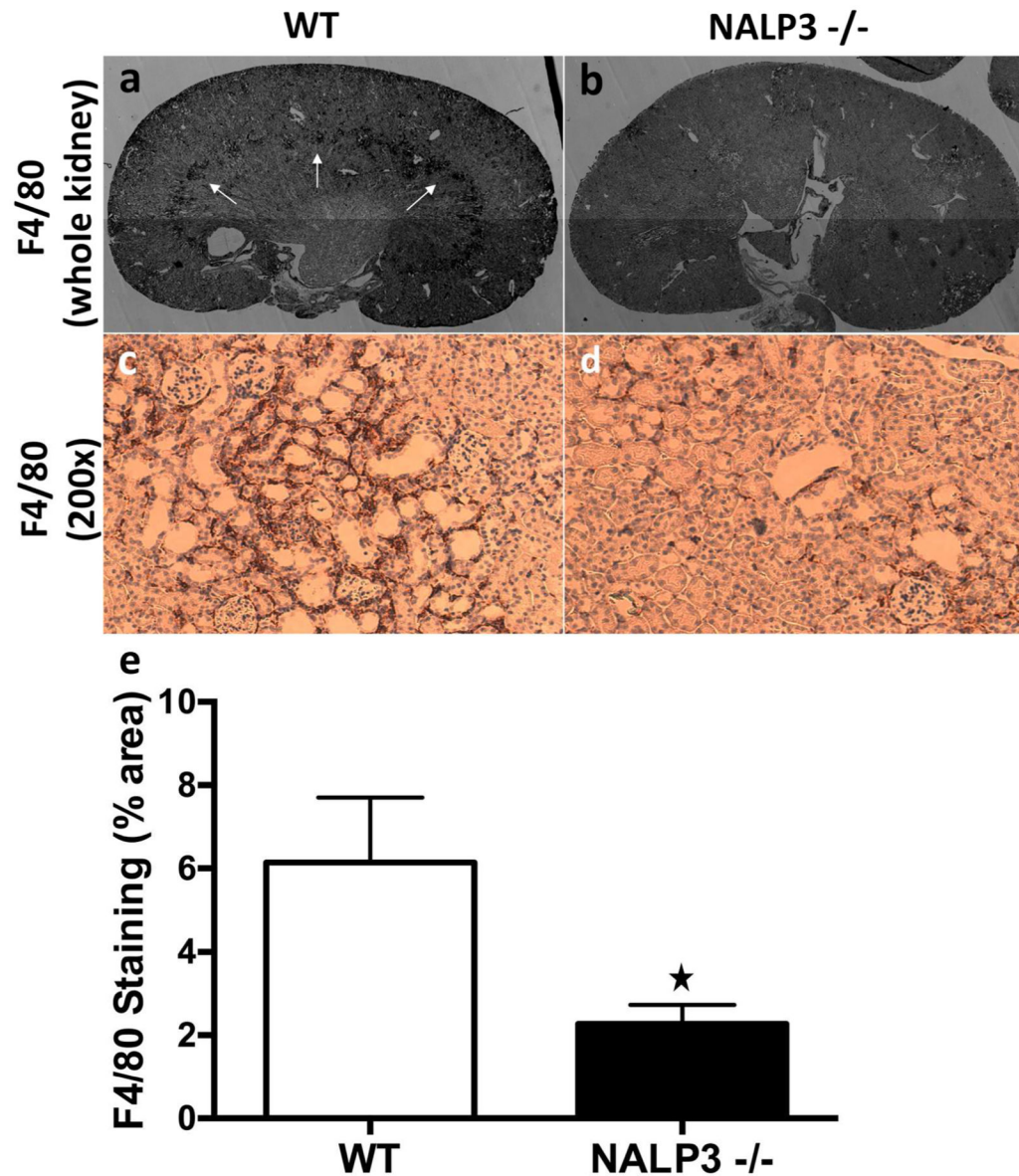


Figure 7. *Nalp3*-deficiency reduces but does not eliminate renal inflammation

(a) F4/80 staining of whole mouse kidneys (dark staining as indicated by white arrows) of wild-type mice fed a high oxalate diet in the absence of calcium demonstrated increased F4/80 staining in wild-type as compared with (b) *Nalp3*-null mice at 6 days. Higher magnification (200x) confirmed more abundant F4/80 staining for macrophages/monocytes in wild-type mice fed a high oxalate diet in the absence of calcium (c) as compared with (d) *Nalp3*-null mice at 6 days (e) Inflammation quantification expressed per kidney surface area in wild-type and *Nalp3*-null mice. Data expressed as the means \pm SEM; n=4 male mice per group; $p < 0.05$. Representative images are shown.

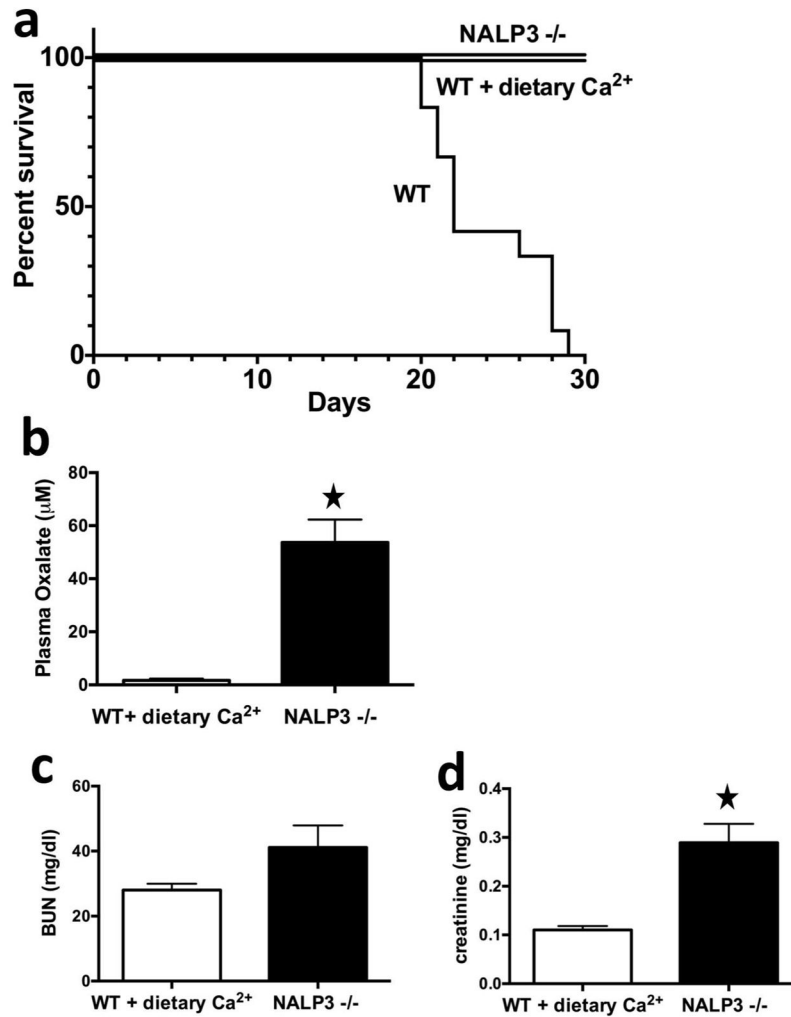


Figure 8. *Nalp3*-deficiency protects from oxalate diet induced mortality

(a) Wild-type mice placed on a diet high in soluble oxalate demonstrated 100% mortality at 30 days. In contrast, *Nalp3*-deficiency or the addition of dietary calcium results in 100% survival at 30 days. Data expressed as Kaplan-Meier Survival Curve; n=12 (6 male/6 female) *Nalp3*-null and wild-type mice fed the diet high in soluble oxalate; n=6 (3 male/3 female) wild-type mice fed high oxalate with calcium (P < 0.0001 for WT vs. *NALP3* -/- and WT with added dietary calcium). (b) Dietary calcium protects from hyperoxalemia in wild-type mice while *Nalp3*-null mice fed a diet high in soluble oxalate had persistent hyperoxalemia at 30 days. (c) BUN and (d) creatinine was compared between wild-type mice placed on a high oxalate diet in the presence of dietary calcium and *Nalp3*-null mice fed a diet high in soluble oxalate for 30 days. Data b-d expressed as the means ± SEM; n=6 (3 male/3 female) for wild-type mice with added dietary calcium and n=12 (6 male/6 female) for *Nalp3*-null mice fed a diet high in soluble oxalate; p < 0.05.